PNAS RESEARCH ARTICLE | NEUROSCIENCE

The circadian molecular clock in the suprachiasmatic nucleus is necessary but not sufficient for fear entrainment

Ivana L. Bussi[a], Miriam Ben-Hamo[a], Luis E. Salazar Leon[a], Leandro P. Casiraghi[a,1], Victor Y. Zhang[a], Alexandra F. Neitz[a,b], Jeffrey Lee[a], Joseph S. Takahashi[c,d], Jeansok J. Kim[e], and Horacio O. de la Iglesia[a,b,2]

Edited by Amita Sehgal, University of Pennsylvania Perelman School of Medicine, Philadelphia, PA; received September 28, 2023; accepted February 22, 2024

We show that nocturnal aversive stimuli presented to mice while they are eating and drinking outside of their safe nest can entrain circadian behaviors, leading to a shift toward daytime activity. We also show that the canonical molecular circadian clock is necessary for fear entrainment and that an intact molecular clockwork in the suprachiasmatic nucleus, the site of the central circadian pacemaker, is necessary but not sufficient to sustain fear entrainment of circadian rhythms. Our results demonstrate that entrainment of a circadian clock by cyclic fearful stimuli can lead to severely mistimed circadian behavior that persists even after the aversive stimulus is removed. Together, our findings support the interpretation that circadian and sleep symptoms associated with fear and anxiety disorders are, in part, the output of a fear-entrained clock, and provide a mechanistic insight into this clock.

fear | suprachiasmatic | circadian | sleep | PTSD

The coding of threatening and aversive stimuli as fear represents a highly conserved adaptation shared across most animals, including humans. For prey species, the ability to encode complex spatial and temporal predator cues, whether innate or learned, is an essential survival mechanism. Likely, the 24-h structure of a predator's activity serves as a crucial temporal cue to its prey. Studies on wild animal populations have indeed shown that the 24-h activity patterns of prey species can be influenced by their predators' activity patterns (1–6). While the mechanisms underlying this temporal predator avoidance are unknown, we have previously shown that nocturnal fear can entrain circadian rhythms of foraging and feeding. Rats living in a safe nest, when required to obtain food and water by venturing into a separate foraging area, predominantly feed and drink during their usual nocturnal phase. However, when the foraging area is made dangerous through randomly distributed footshocks during the dark phase of the light–dark (LD) cycle, the rats shift their feeding and drinking activities to the daytime (7).

This unusual diurnal behavior observed in a nocturnal rodent could have emerged either as an avoidance response to nocturnal footshocks or as a result of learning wherein the light phase becomes conditionally associated with safety. However, our studies showed that rats can anticipate the safe light phase and begin venturing into the foraging area, initiating eating and drinking activities at the end of the dark phase, before lights turn on signaling the safe time of day. This finding suggested the potential involvement of a circadian clock in predicting the cyclic aversive stimulus. Indeed, we have shown that rhythms of activity in the foraging area and feeding resulted from the entrainment of a circadian oscillator (7). The reliance of this oscillator on the canonical molecular circadian clock and the timing by the central circadian pacemaker located within the suprachiasmatic nucleus (SCN) is yet to be determined. Here, we exploit our fear-entrainment paradigm in mice to a) show that cyclic fear entrainment is likely a conserved feature of the circadian system of mammals, b) reveal basic properties of entrainment by cyclic fear, c) confirm that the fear-entrained oscillator depends on the canonical molecular clock, and d) demonstrate that an intact molecular clock within the SCN is necessary, though not sufficient, for fear entrainment. Our findings underscore the salience of cyclic 24-h fear stimuli as a key entraining environmental cycle for the circadian system that has the ability to drastically shift the temporal distribution of behavior, providing a neural framework to understand circadian and sleep disruptions associated with fear and anxiety disorders.

Results

Nocturnal Fear Entrains Circadian Rhythms of Foraging and Feeding Behavior in the Mouse. To assess whether a fearful stimulus can entrain circadian rhythms of locomotor activity in the mouse, we first built customized cages that mimic a more naturalistic

Significance

Cyclic fearful stimuli presented while mice are foraging and feeding outside of a safe nest can entrain circadian rhythms and lead to predominantly diurnal activity; this mistimed circadian behavior persists for days after the aversive stimulus is no longer present. Our results suggest that disrupted circadian rhythms and sleep typical of anxiety disorders, such as posttraumatic stress disorder, may represent the output of a previously entrained fear-entrained circadian clock whose output sustains a maladaptive timing of behavior and sleep in the absence of actual threats. We provide mechanistic insight into this fear-entrained clock, which could contribute to the elucidation of molecular mechanisms and neural circuitry that underlie anxiety disorders and provide broad avenues for their treatment.

Author contributions: I.L.B., M.B.-H., J.J.K., and H.O.d.l.I. designed research; I.L.B., M.B.-H., L.E.S.L., L.P.C., V.Y.Z., A.F.N., J.L., and H.O.d.l.I. performed research; I.L.B., L.P.C., A.F.N., J.S.T., J.J.K., and H.O.d.l.I. contributed new reagents/analytic tools; I.L.B., M.B.-H., L.E.S.L., L.P.C., V.Y.Z., A.F.N., and H.O.d.l.I. analyzed data; M.B.-H., L.E.S.L., L.P.C., V.Y.Z., A.F.N., J.L., J.S.T., and J.J.K. revised manuscript; and I.L.B. and H.O.d.l.I. wrote the paper.

The authors declare no competing interest.

This article is a PNAS Direct Submission.

[1]Present address: Laboratorio Interdisciplinario del Tiempo, Escuela de Educación, Universidad de San Andrés/Consejo Nacional de Investigaciones Científicas y Técnicas (CONICET), Buenos Aires B1644BID, Argentina.

[2]To whom correspondence may be addressed. Email: horaciod@uw.edu.

This article contains supporting information online at https://www.pnas.org/lookup/suppl/doi:10.1073/pnas.2316841121/-/DCSupplemental.

Published March 19, 2024.

environment than regular housing cages. These cages have two different compartments: a nesting compartment where the mice are safe from the aversive stimulus and a foraging area where food and water are available ad libitum but where footshocks can be delivered through a metal grid floor (*SI Appendix*, Fig. S1*A*). These cages allowed us to record three different behavioral outputs: locomotor activity within the nesting area (hereafter referred to as "nest activity") and within the foraging area (hereafter referred to as "foraging") with IR detectors, and feeding through a nose-poke detector in the feeder.

Adult male and female mice were housed in these customized cages and subjected to a 12:12 LD schedule. After 10 d in baseline conditions, we started delivering three footshocks per hour—randomly distributed throughout time—in a 12-h time window within either the dark (dark fear = DF) or the light (light fear = LF) phase of the LD cycle. LF mice displayed a mild change in behavior after the presentation of the shocks, avoiding the daytime activity evident during baseline (Fig. 1 *A*, *Left* panel and *SI Appendix*, Fig. S1*B*). In contrast, DF mice progressively shifted their nocturnal activity to the light phase, with most of the activity occurring during the first hours of the light phase (Fig. 1 *A*, *Right* panel and *SI Appendix*, Fig. S1*E*). DF mice also showed increased activity during the last hour of darkness before lights-on, which we interpret as anticipation of the shock-free phase. Waveform analysis including all animals in each group confirmed the nocturnal and diurnal activity patterns, respectively, of LF and DF animals (Fig. 1*B* and *SI Appendix*, Fig. S1 *C* and *F*).

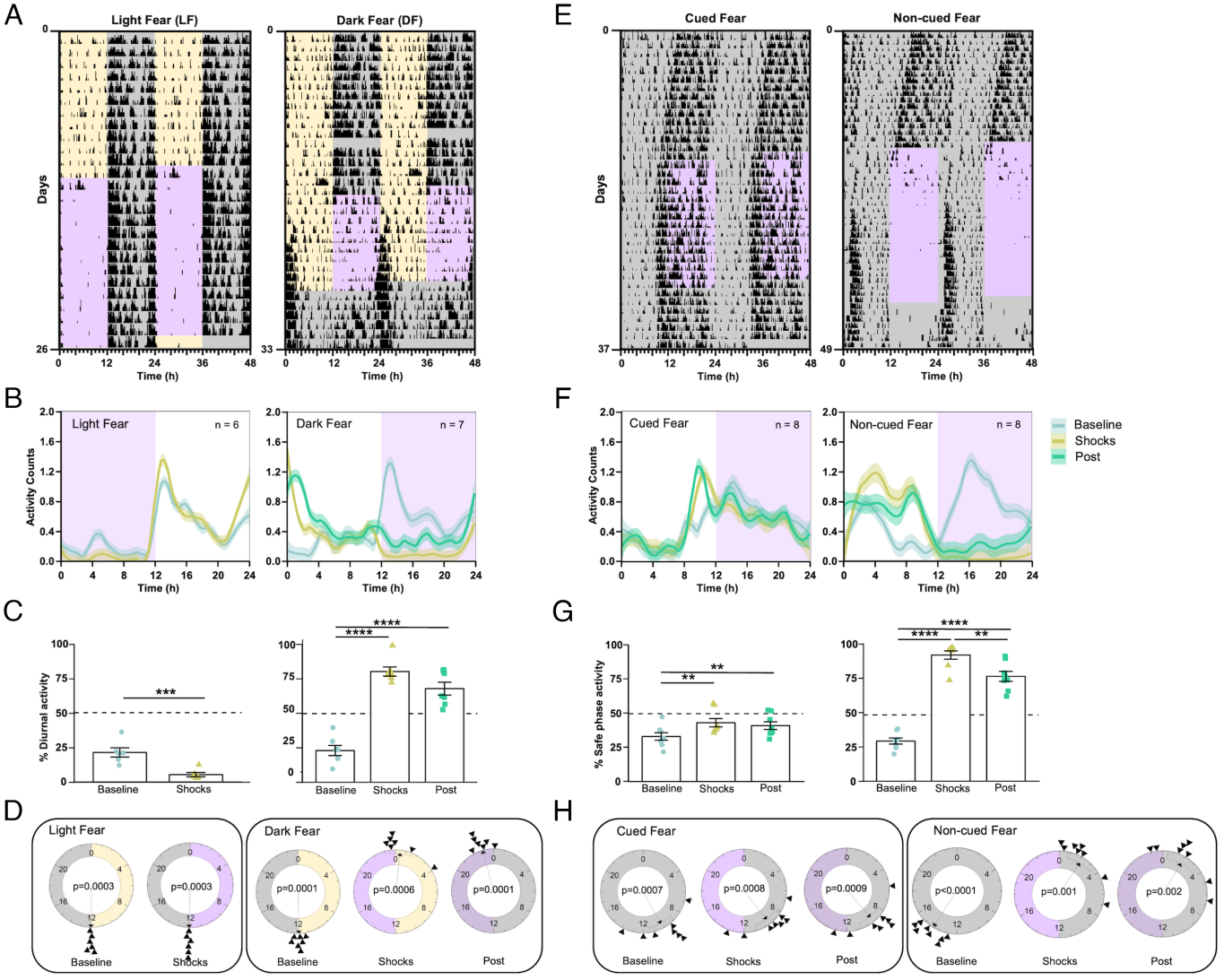

Fig. 1. Cyclic fear entrains a circadian oscillator under a LD cycle or constant darkness. (*A*) Representative foraging actograms from mice in LD subjected to cyclic fear presented either during the day (LF, *Left*) or during the night (DF, *Right*). Yellow and gray shading, respectively, represents the light and dark phases of a 12:12 LD cycle. Purple shading represents the 12-h window of time at which 3 footshocks/h randomly distributed over time were presented. The DF mouse is released into constant conditions (DD and no shocks). (*B*) Average foraging activity patterns (line represents locally estimated scatterplot smoothing (LOESS) regressions obtained from the mean values of all mice mean and shading SEM) from mice under LF (*Left*, n = 6) or DF (*Right*, n = 7). (*C*) Percent of activity that took place during the daytime or extrapolated daytime across the different experimental stages from the same mice shown in *B*. Bars represent the mean ± SEM. (*D*) Rayleigh plots representing the time of activity onset across the different experimental stages for mice subjected to LF (*Left*) or DF (*Right*). (*E*) Representative foraging actograms from mice in DD subjected to either cued (*Left*) or noncued (*Right*) fear during the subjective night. Purple shading represents the shock-delivering window. (*F*) Average foraging activity patterns from mice subjected to cued (*Left*, n = 8) or noncued fear (*Right*, n = 8). (*G*) Percent of activity that took place during the safe phase (window of time without shocks) or extrapolated safe phase across the different experimental stages from the same mice shown in *F*. (*H*) Rayleigh plots representing the time of the activity onset during the different stages of the protocol for mice subjected to cued (*Left*) or noncued fear (*Right*). Asterisks indicate statistically significant differences according to Tukey comparisons following LMM analysis (*SI Appendix*, Table S1): $^{**}P < 0.01$, $^{***}P < 0.001$.

To test whether the daytime activity of DF mice represented an acute response to the dark-phase shocks, we released DF mice into constant darkness conditions (DD) in the absence of footshocks (hereafter referred to as postshocks). Upon release into constant conditions, the phase of the rhythms of foraging, feeding, and, to some extent, nest activity resembled the phase during the presentation of the shocks, indicating that the daytime activity was the result of authentic entrainment by the nocturnal footshocks (Fig. 1 *A*, *Right* panel and *SI Appendix*, Fig. S1*E*). Waveform analysis of all three behaviors confirmed the phase of DF mice after their release into constant conditions (Fig. 1 *B*, *Right* panel and *SI Appendix*, Fig. S1*F*).

We analyzed these data as follows: First, we determined the percent of diurnal activity for each of the three behavioral outputs within each animal. Then, we analyzed this variable through linear models with mixed effects (LMM), with the group (LF vs. DF) and experimental stage (baseline, shocks, or postshocks) as fixed factors and the individual mouse as a random factor (*SI Appendix*, Table S1). This analysis revealed that LF mice displayed less diurnal activity during the presentation of shocks than during baseline (Fig. 1 *C*, *Left* panel and *SI Appendix*, Fig. S1*C*). For instance, 21.4 ± 3.3% (mean±SEM) of the foraging activity occurred during the daytime on baseline, but only 5.4 ± 1.5% occurred during the daytime when shocks were delivered (Fig. 1 *C*, *Left* panel). The analysis also revealed that DF animals switched from being predominantly nocturnal in all three behaviors during baseline to being predominantly diurnal during the presentation of shocks as well as upon their release into constant conditions (Fig. 1 *C*, *Right* panel and *SI Appendix*, Fig. S1*F*). For instance, 23.3 ± 3.7% of the foraging activity occurred during the daytime on baseline, 80.5 ± 4.7% occurred during the daytime when shocks were delivered, and 68.1 ± 4.7% during the projected daytime after their release into constant conditions (Fig. 1 *C*, *Right* panel).

Second, we used circular statistics to assess the changes in the phase of the 24-h onset of foraging activity. Circular plots of the onset of each animal's foraging time are presented in Fig. 1*D*, and their analysis through the Rayleigh test is in *SI Appendix*, Table S2. This analysis revealed that LF animals started foraging at the time of lights-off during baseline, and this phase remained during the presentation of shocks. In contrast, although DF animals also started foraging at the time of lights-off during baseline, they shifted by approximately 12 h during the presentation of shocks, with the phase of the foraging start time occurring around lights-on and coincident with the termination of the daily shocks. Importantly, this latter phase remained when the animals were released into constant conditions.

Cyclic Fear Entrains Circadian Rhythms of Foraging and Feeding Behavior Under Constant Darkness Conditions. Our fear-entrainment paradigm under LD conditions presents the confounding effect that footshocks in both groups are always paired with a particular phase of the LD cycle, raising the possibility that cyclic fear could only entrain circadian rhythms when an external time reference is present. To test whether this is the case, we repeated our experiment under DD. During a ~12-d baseline phase in which animals were placed in the fear chambers under DD, mice displayed the typical <24-h circadian period in rhythms of foraging, feeding, and nest activity (Fig. 1*E* and *SI Appendix*, Fig. S2 *A* and *D*). After the baseline phase, the control group received three footshocks per hour—randomly distributed throughout time—during a 12-h time window, but these shocks were preceded by a 20-s tone (*cued-fear*), which allowed the animals to predict the arrival of the footshock. The experimental group received the same temporal distribution of footshocks, but the shocks were not paired with a tone (*noncued fear*). The results showed that cued-fear mice effectively predicted and avoided the shocks and did not change the circadian phase of any of the three behavioral outputs measured (Fig. 1 *E*, *Left* panel and *SI Appendix*, Fig. S2*A*). In contrast, noncued-fear animals shifted their rhythms within a few cycles, leading to a pattern of foraging, feeding, and nest activity that effectively avoided activity during the shock phase (Fig. 1 *E*, *Right* panel and *SI Appendix*, Fig. S2*D*). Importantly, upon release into constant conditions (with no shocks), both groups displayed a circadian phase that was predicted by the phase displayed during the presentation of shocks. Waveform analysis confirmed the 24-h temporal pattern of all three behaviors in both cued and noncued mice (Fig. 1*F* and *SI Appendix*, Fig. S2 *B* and *E*).

We determined the percent of activity for each of the three behavioral outputs that took place during the safe phase (the 12-h window without footshocks) within each animal and analyzed the change in this variable across stages through an LMM. In cued-fear animals, during the presentation of shocks, the percent of each behavior displayed during the safe phase differed slightly relative to the percent activity in the extrapolated phase during baseline and continued to differ slightly from baseline when the shocks were removed (Fig. 1 *G*, *Left* panel and *SI Appendix*, Fig. S2*C* and Table S1). These slight changes in phase were likely the consequence of the fact that the animals exhibited a different period than the 24-h period of the cyclic cued shocks. In contrast, the percent of activity during the safe phase in mice subjected to the noncued fear protocol changed dramatically during the presentation of shocks (94.6% for foraging, 96.4% for feeding, and 63.5 for nest activity) when compared to the percent of activity in the extrapolated phase during the baseline (30.5% for foraging, 30.9% for feeding, and 36.2% for nest activity). These results clearly revealed that all three behaviors were largely restricted to the safe phase of the 24-h shock cycle. The trend persisted when shocks were removed, with a large percent of each behavior restricted to the extrapolated safe phase during the postshocks stage (78.7% for foraging, 84.9% for feeding, and 50.5 for nest activity; Fig. 1 *G*, *Right* panel and *SI Appendix*, Fig. S2*F* and Table S1). Circular plots followed by the Rayleigh tests clearly showed that while the phase of rhythmic foraging in cued-fear animals did not shift with the presentation of shocks, the rhythm was readily entrained by the presentation of shocks in noncued fear animals, in which the onset of activity occurred right after the time the shock window ended (Fig. 1*H* and *SI Appendix*, Table S2).

Circadian Clock Gene Expression in the Suprachiasmatic Nucleus Is Not Entrained by Cyclic Fear. Entrainment of circadian rhythms by cyclic nocturnal fear could be the result of entrainment of the central circadian clock housed within the SCN. To test this possibility, we performed in situ hybridization for the clock genes *Bmal1* and *Per1* in coronal brain slices from either LF or DF mice killed every 4 h throughout the 24-h cycle. The pattern of *Bmal1* and *Per1* expression in both groups was indistinguishable and showed the expected circadian expression that would result from photic entrainment of the SCN, i.e., respectively high and low expression of *Per1* and *Bmal1* during the light phase (Fig. 2). Cosinor analysis followed by a Wald test confirmed there were no detectable differences in the amplitude or phase of clock gene expression patterns between LF and DF animals (*SI Appendix*, Table S3). Because of their involvement in contextual fear-conditioning, we also examined the pattern of clock gene expression in the dentate gyrus of the hippocampus (DG) and basolateral amygdala (BLA). The cosinor analysis failed to detect any rhythm in the expression of the *Per1* gene in the BLA or DG for LF or DF samples (*SI Appendix*, Fig. S3 and Table S3).

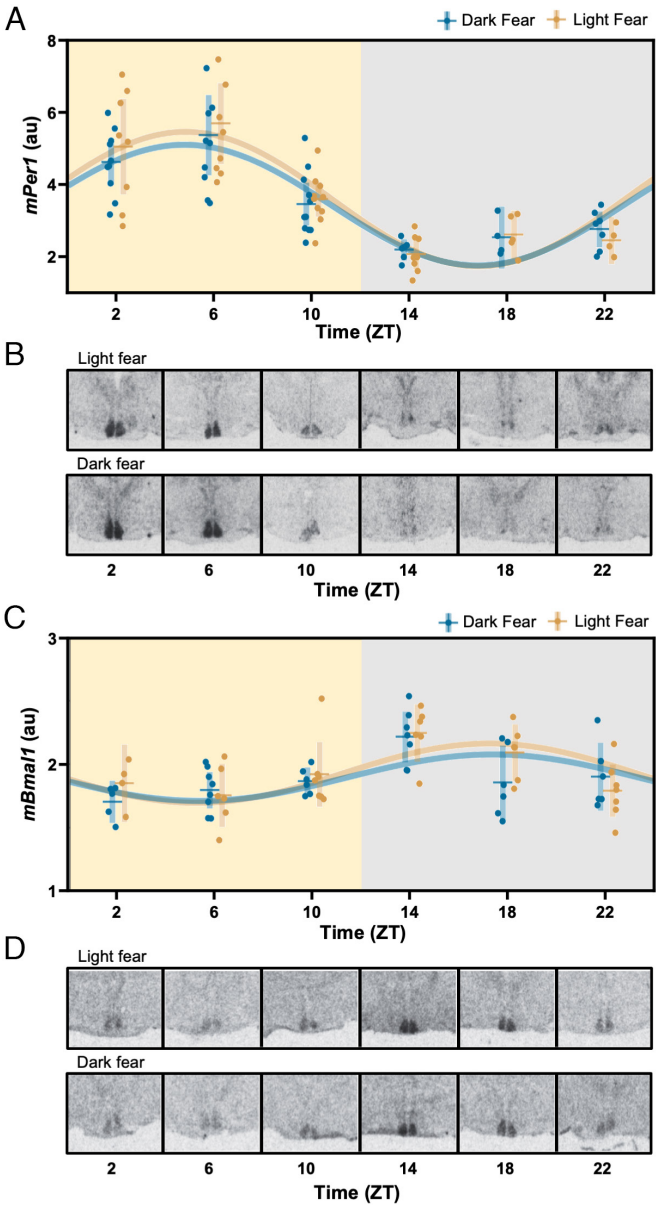

Fig. 2. Circadian clock gene expression in the SCN is entrained to the LD cycle independently of fear entrainment. (*A–D*) Daily patterns of *mPer1* and *mBmal1* mRNA expression, respectively, in mice housed under a 12:12 LD cycle subjected to LF or DF. In *A* and *C*, each dot represents an individual mouse, horizontal and vertical lines, respectively, represent the mean and SEM. The best-fitting sine wave with a 24-h period for each group is presented for illustrative purposes (solid lines, fit parameters are presented in *SI Appendix*, Table S3). *B* and *D* show representative autoradiographs of coronal brain sections at the level of the anterior hypothalamus, hybridized with a radioactive probe for *mPer1* and *mBmal1* mRNA detection, respectively.

The Expression of the Clock Gene *Bmal1* in the Forebrain Is Necessary for Fear Entrainment. The central regulation of overt behavioral and physiological rhythms in mammals relies on the transcription-translation feedback loop of canonical clock genes within cells of the SCN (8, 9). However, several studies have shown that behavioral circadian rhythms entrained to time-restricted food access do not rely either on the SCN or the canonical molecular clockwork (10–12). We reasoned that this independence from the SCN molecular clockwork could be a characteristic of nonphotically entrained circadian rhythms and examined whether the circadian canonical clock is necessary to sustain fear-entrained circadian rhythms. We tested mice lacking the clock gene *Bmal1* in the forebrain, which readily entrain to time-restricted food access (12), in our fear-entrainment paradigm. In this mouse line, a Cre-driver under the promoter of the *CamKII* gene targets the deletion of *Bmal1* to neurons within structures within the forebrain and leads to rhythmic behavior under LD driven by masking—the expression of rhythmic behavior as mere response to the LD cycle—but to arrhythmic locomotor activity patterns under DD in mice lacking both copies of the gene. However, a single copy of *Bmal1* in the forebrain is sufficient to sustain behavioral circadian rhythmicity (12).

We tested mice lacking either both copies of *Bmal1* (*Cami-Bmal1*$^{-/-}$), only one copy of *Bmal1* (*Cami-Bmal1*$^{+/-}$) or none (*Cami-Bmal1*$^{+/+}$) under DF and noncued fear protocols. In LD and during baseline conditions, *Cami-Bmal1*$^{-/-}$, *Cami-Bmal1*$^{+/-}$, and *Cami-Bmal1*$^{+/+}$ displayed nocturnal activity. When subjected to DF, the three groups successfully shifted their behaviors to the light phase, indicating that the lack of *Bmal1* expression does not impair fear perception. Upon release into constant conditions (DD and no footshocks), *Cami-Bmal1*$^{+/-}$ and *Cami-Bmal1*$^{+/+}$ mice maintained the phase acquired during the shock-presentation phase (Fig. 3*A* and *SI Appendix*, Fig. S4*A*). In contrast, *Cami-Bmal1*$^{-/-}$ displayed an arrhythmic pattern of behavior, suggesting that the synchronization during the shock presentation phase was the result of pairing the aversive stimulus to the dark phase instead of the entrainment of a functional circadian clock (Fig. 3*A* and *SI Appendix*, Fig. S4*A*). Waveform analysis confirmed the results for each group, and also revealed that the *Cami-Bmal1*$^{-/-}$ group displayed lower levels of foraging during the presentation of shocks than after release into constant conditions (Fig. 3*B*). The LMM analysis of the percentage of each behavior that took place during the daytime or the extrapolated daytime yielded an effect of genotype for nest activity, an effect of experimental stage (baseline, shock presentation, or constant conditions), and an interaction for all three behaviors (*SI Appendix*, Table S4). Tukey post hoc comparisons showed statistically significant differences between the different stages of the experiment for all genotypes, indicating that all animals avoided the dark-phase shocks. Visual inspection of the actograms (Fig. 3*A* and *SI Appendix*, Fig. S4*A*) as well as analysis of the percentage of activity during the light phase (no shocks) and the projected light phase (Fig. 3*C* and *SI Appendix*, Fig. S4*B*) revealed that mice with at least one copy of *Bmal1* entrained to the nocturnal fear. In contrast, *Cami-Bmal1*$^{-/-}$ mice avoided the shocks, but this was the result of masking, as they became arrhythmic immediately upon release into constant conditions.

To determine how the rhythmicity of each of the three behaviors changed throughout the stages of the experiment, we calculated the amplitude of the fast-Fourier transform (FFT) in a circadian range, which provides an estimate of the robustness of a rhythm. We then fitted a LMM with experimental stage, genotype, and their interaction as fixed factors, and the individual mouse as a random factor. The model yielded an effect of the experimental stage for all three behaviors but no detectable effects of genotype or interaction, revealing the effect of the nocturnal shocks on mice of all genotypes. Most importantly, the apparent lack of any amplitude peak in the circadian frequencies for *Cami-Bmal1*$^{-/-}$ mice confirmed their lack of circadian rhythmicity after their release into constant conditions (Fig. 3*D* and *SI Appendix*, Fig. S4*D* and Table S5).

To assess the effect of a dysfunctional molecular clock on fear entrainment under DD, *Cami-Bmal1*$^{-/-}$ mice and their littermate controls were subjected to the noncued fear protocol in DD. *Cami-Bmal1*$^{+/-}$ and *Cami-Bmal1*$^{+/+}$ mice were able to avoid the shocks by shifting their activity to the safe time of the day and

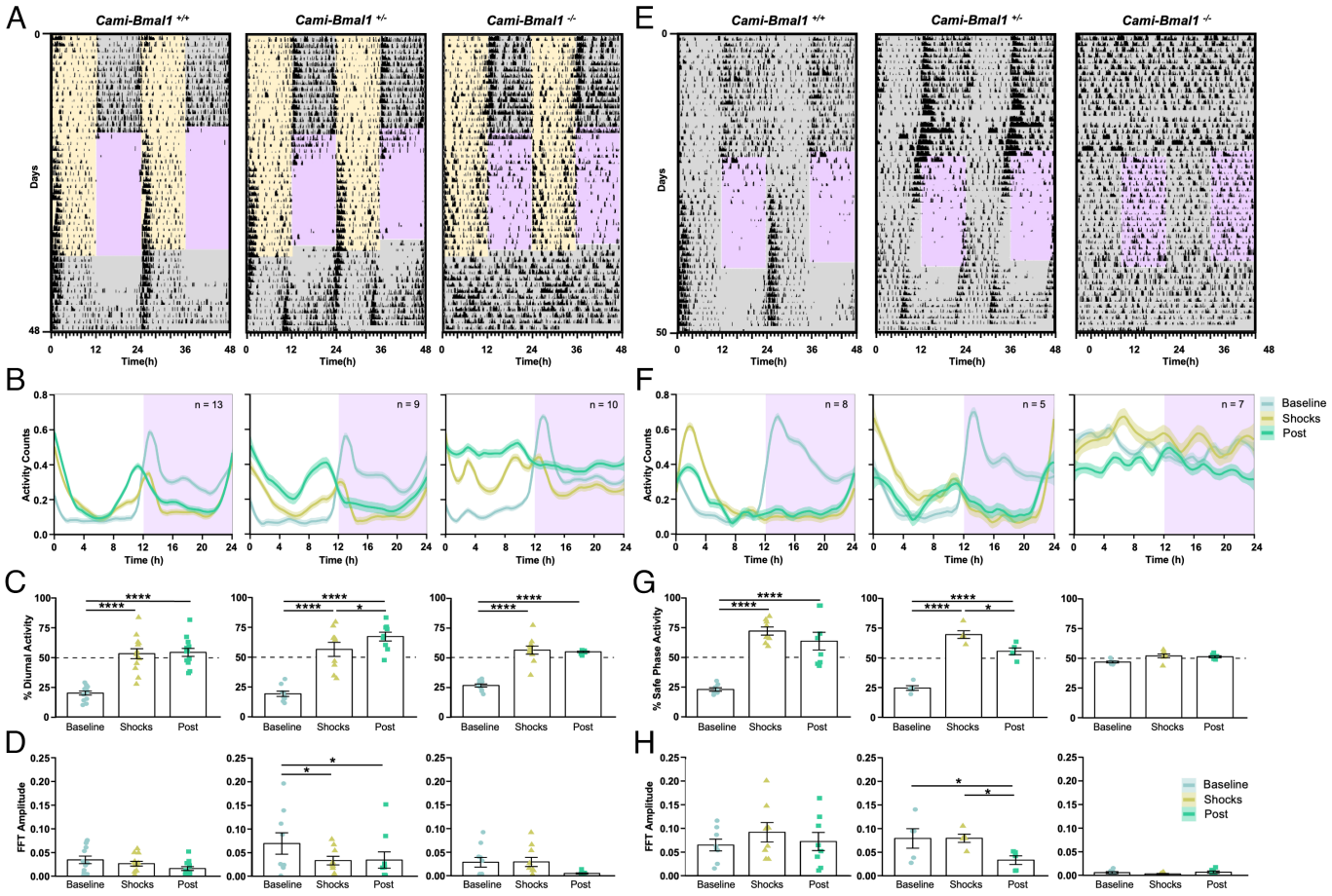

Fig. 3. The expression of the clock gene *Bmal1* in the forebrain is necessary for fear entrainment. (*A*) Representative foraging actograms from *Cami-Bmal1*$^{+/+}$, *Cami-Bmal1*$^{+/-}$, and *Cami-Bmal1*$^{-/-}$ mice subjected to DF. (*B*) Average activity patterns from *Cami-Bmal1*$^{+/+}$ (*Left*, n = 13), *Cami-Bmal1*$^{+/-}$ (*Center*, n = 9), and *Cami-Bmal1*$^{-/-}$ mice (*Right*, n = 10) in LD subjected to DF. (*C*) Percentage of activity during the daytime or extrapolated daytime across the different experimental stages from the same mice shown in *B*. (*D*) Fast-Fourier transform (FFT) amplitude across the successive stages from the same mice shown in *B*. (*E*) Representative foraging actograms from *Cami-Bmal1*$^{+/+}$, *Cami-Bmal1*$^{+/-}$, and *Cami-Bmal1*$^{-/-}$ mice subjected to a 12-h window of noncued fear under DD. (*F*) Average activity patterns from *Cami-Bmal1*$^{+/+}$ (*Left*, n = 8), *Cami-Bmal1*$^{+/-}$ (*Center*, n = 5), and *Cami-Bmal1*$^{-/-}$ mice (*Right*, n = 7) subjected to noncued fear in DD. (*G*) Percent of activity that took place during the safe phase (window of time without shocks) or extrapolated safe phase across the different experimental stages from the same mice shown in *F*. (*H*) FFT amplitude across the successive stages from the same mice shown in *F*. Asterisks indicate statistically significant differences according to Tukey comparisons following LMM analysis: *P < 0.05, **P < 0.01, ***P < 0.001, ****P < 0.0001.

displayed the expected phase upon release into constant conditions (Fig. 3 *E* and *F* and *SI Appendix*, Fig. S5 *A* and *B*, *Left* and *Center* panels). Remarkably, *Cami-Bmal1*$^{-/-}$ mice maintained their arrhythmic pattern during the entire protocol and, during the shock presentation phase, were unable to avoid the shocks by timing their activity to the nonshock phase, suggesting an inability to determine when the aversive stimulus occurred (Fig. 3 *E* and *F* and *SI Appendix*, Fig. S5 *A* and *B*, *Right* panels). This conclusion was further supported by the LMM analysis of the percentage of activity that took place during the safe time of the day (Fig. 3*G* and *SI Appendix*, Fig. S5*C* and Table S6) and of the FFT amplitude (Fig. 3*H* and *SI Appendix*, Fig. S5*D* and Table S7). This latter analysis revealed that *Cami-Bmal1*$^{-/-}$ mice lacked amplitude peaks in the circadian frequencies throughout all stages of the experiment.

An Intact Molecular Circadian Clock Within the Suprachiasmatic Nucleus Is Necessary but Not Sufficient to Sustain Fear-entrained Circadian Rhythms. Our results in *Cami-Bmal1*$^{-/-}$ mice clearly point to the necessity of an intact molecular circadian clock in the forebrain to sustain cyclic fear entrainment. However, they do not have the regional specificity to determine in which areas of the forebrain clock gene expression is critical for fear entrainment. Specifically, we wondered whether clock gene expression within the SCN central clock is necessary and/or sufficient to sustain fear entrainment of behavioral rhythms.

To test this, we injected a Cre-expressing virus (AAV2/1-Ef1a-Gfp-Cre) into the SCN of *Bmal1*$^{fx/fx}$ mice to delete the *Bmal1* gene specifically from this brain region (Fig. 4*A*). Mice with off-target injections (no trace of the virus near the SCN) served as controls. As expected, mice lacking *Bmal1* in the SCN (SCN-*Bmal1*$^{-/-}$) became arrhythmic in DD shortly after the viral injection (*SI Appendix*, Fig. S6 *A* and *B*). When subjected to the noncued fear-entrainment paradigm under DD, SCN-*Bmal1*$^{-/-}$ continued to display an arrhythmic pattern of locomotor activity throughout the protocol, displaying a reduction in the locomotor activity during the shock-presentation window, indicating that these mice were able to sense the aversive nature of the shocks (Fig. 4 *B*, *Center* panel). In one case, the cyclic fear induced a small degree of activity consolidation in the nonfear phase and a free-running pattern of activity that was coincident with the phase acquired during the shocks (Fig. 4 *B*, *Right* panel). This result suggests that the viral injection spared a small proportion of SCN cells that may have been sufficient for entrainment when forced by the cyclic fearful stimulus presentation. However, we included this mouse in the SCN-*Bmal1*$^{-/-}$ group based on the histological results (see *SI Appendix*, Fig. S6*B* for an example of histological

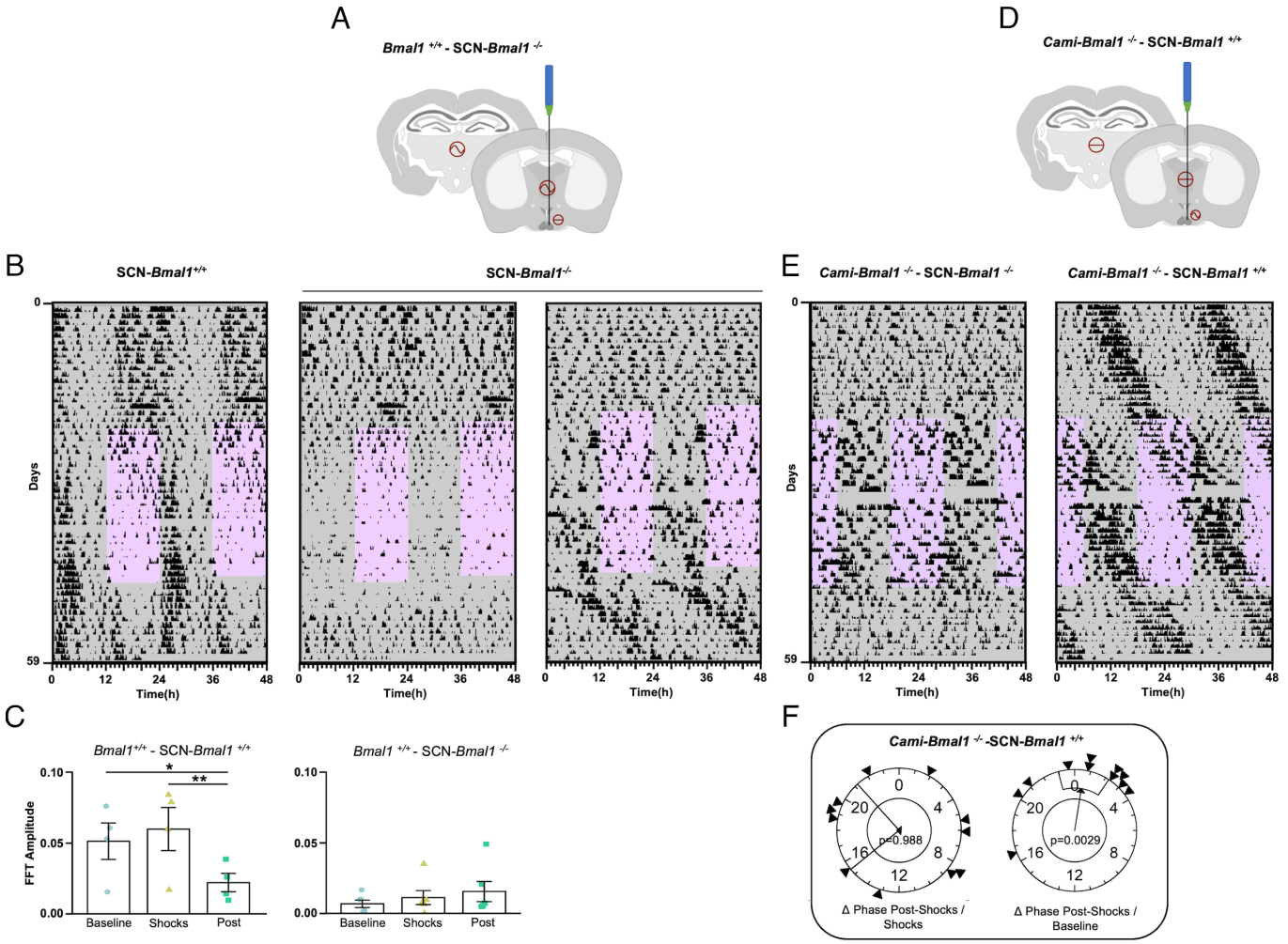

Fig. 4. The circadian canonical clock within the SCN is necessary but not sufficient for fear entrainment. (*A*) Schematic representation of the genetic strategy used to knock out *mBmal1* in the SCN. A *Bmal1*$^{fx/fx}$ mouse is bilaterally injected with a Cre-expressing AAV in the SCN. (*B*) Representative foraging actograms from an SCN-*Bmal1*$^{+/+}$ control mouse (*Left*) and two SCN-*Bmal1*$^{-/-}$ mice (*Center* and *Right*) subjected to cyclic fear under DD. (*C*) FFT amplitude across the successive experimental stages from SCN-*Bmal1*$^{+/+}$ mice (*Left*, n = 4) and SCN-*Bmal1*$^{-/-}$ mice (*Right*, n = 6). (*D*) Schematic representation of the genetic strategy to rescue *Bmal1* expression in the SCN. A *Cami-Bmal1*$^{-/-}$ mouse is bilaterally injected with Cre-dependent *Bmal1*-expressing AAV. (*E*) Representative foraging actograms from *Cami-Bmal1*$^{-/-}$-SCN-*Bmal1*$^{-/-}$ mouse (*Left*) and *Cami-Bmal1*$^{-/-}$-SCN-*Bmal1*$^{+/+}$ mouse (*Right*) subjected to the noncued fear protocol in DD. (*F*) Rayleigh plots representing the phase of activity onset in the postshock phase of *Cami-Bmal1*$^{-/-}$-SCN-*Bmal1*$^{+/+}$ mice relative to the shock phase (*Left*) or to the baseline phase (*Right*). Asterisks indicate statistically significant differences according to Tukey comparisons following LMM analysis: *$P < 0.05$, **$P < 0.01$.

staining) and the arrhythmicity shown during the baseline stage. The FFT amplitude in the circadian range was quantified at each stage of the protocol as an indicator of the robustness of the rhythm. Control animals showed an overall reduction in FFT amplitude during the postshock stage relative to the baseline and the shock presentation stage (Fig. 4 *B* and *C* and *SI Appendix*, Fig. S6 *C* and *D*, *Left* panels, and Table S8). SCN-*Bmal1*$^{-/-}$ showed a lower amplitude FFT throughout all stages of the protocol. Interestingly, for the mouse whose actogram is shown in Fig. 4 *B*, *Right* panel, the FFT amplitude increased progressively through the experimental stages, suggesting that a few cells retaining clock genes in the SCN may have been recruited by the fear entrainment. In summary, our results show that a functional circadian clock within the SCN is necessary to sustain fear-entrained circadian rhythms.

To test whether clock gene expression within the SCN is sufficient to sustain fear-entrained circadian rhythms, we used a complementary approach. We rescued the expression of *Bmal1* in the SCN of mice lacking this gene in the forebrain (*Cami-Bmal1*$^{-/-}$), which were unable to entrain to cyclic fear in DD, by injecting a Cre-dependent *Bmal1*-expressing AAV (AAV2/1-Ef1a-DIO-Bmal1; Fig. 4*D*). This strategy rescues *Bmal1* expression under a constitutive promoter but similar strategies have successfully rescued the molecular clock's ~24-h oscillation in other *Bmal1*$^{-/-}$ systems (13–15).

While control mice with off-target injections showed arrhythmic patterns of locomotor activity in DD, mice injected with the *Bmal1*-expressing virus within the SCN (*Cami-Bmal1*$^{-/-}$- *SCN-Bmal1*$^{+/+}$) recovered the behavioral rhythmicity shortly after the surgery (*SI Appendix*, Fig. S7 *A* and *B*). When these mice were subjected to the noncued fear paradigm, they free-ran through the protocol, ignoring the 12-h shock-presentation phase (Fig. 4 *E*, *Right* panel). In some individuals, a decrease in foraging and feeding was evident during the shock hours (Fig. 4*E* and *SI Appendix*, Fig. S7*C*). Polar plots followed by Rayleigh tests of the rhythm phases showed that the phases of all three behavioral outputs during the postshock stage were predicted by the phases during the baseline and not by the time of shocks (Fig. 4*F* and *SI Appendix*, Fig. S7*D* and Table S9).

To assess whether the inability of Cami-*Bmal1*$^{-/-}$- SCN-*Bmal1*$^{+/+}$ mice to entrain to cyclic fear was specific to this cyclic stimulus or it was related to a limitation caused by the constitutive expression

of *Bmal1* in the rescued mice not being able to fully recapitulate the physiological features of a normal SCN, we recorded their home-cage activity under a 12:12 LD cycle for 10 days and then released them into DD. Under LD, the onset of locomotor activity of *Cami-Bmal1*$^{-/-}$- SCN-*Bmal1*$^{+/+}$ mice displayed small phase changes (transients) until it reached a stable phase after the time of lights-off. Importantly, upon release into DD conditions, the phase of the locomotor activity rhythm remained the same, demonstrating true entrainment to the LD cycle (*SI Appendix*, Fig. S7 *E* and *F*).

Together, these results demonstrate a failure of cyclic fear to entrain the rescued rhythms and therefore that a functional circadian clock within the SCN is not sufficient to sustain fear-entrained circadian rhythms.

Discussion

In the present study, we show that mice living in a more naturalistic environment recreated in the laboratory, where they are required to venture out of their safe nest to obtain food and water, display nocturnal food-seeking and feeding behavior. However, the chronic application of a nocturnal aversive stimulus in the foraging area leads to a shift in foraging and feeding behavior to daytime. This shift results from cyclic fear entrainment of a circadian oscillator, similar to what occurs in rats (7). Our results suggest that cyclic fear is a potent nonphotic entraining environmental cycle or *zeitgeber* for the circadian system, capable of dramatically shifting 24-h patterns of overt behavior. Furthermore, we demonstrate that this fear-entrained oscillator relies on the canonical circadian molecular clock. Using conditional knock-out strategies, we also show that an intact molecular clock within the central circadian clock located in the SCN is necessary but not sufficient to sustain fear entrainment.

Virtually all organisms rely on circadian systems to predict 24-h cyclic events in nature. Internal biological clocks provide a mechanism by which organisms can anticipate these events with changes in physiology and behavior. Because circadian clocks have periods that differ from 24 h, they require entrainment by 24-h environmental cycles. Throughout evolution, the LD cycle has been selected as a highly reliable cycle conveying solar time, and the circadian clocks of most organisms are entrained by it. However, animals live in complex temporal environments, and their circadian system can be entrained by nonphotic zeitgebers as well (16, 17). A classic example of this nonphotic entrainment is time-restricted feeding, which leads to activity in anticipation of feeding events and is the result of entrainment by a food-entrainable oscillator(s) (FEO) (18, 19). Here, we show that cyclic fear is similarly effective in entraining circadian rhythms. Given that the ability of animals to perceive and respond appropriately to threats directly affects individual survival, it is logical that cyclic fear acts as a strong zeitgeber. This adaptive response should reliably reduce the negative fitness consequences of encountering recurring dangers, such as predators, in the wild.

Upon release of DF animals into constant conditions, there is a reemergence of the previous nocturnal activity (Fig. 1*A* and *SI Appendix*, Fig. S1*E*). Although this could be interpreted as the removal of masking by cyclic fear, we do not think this is the case because the reemergence of this activity appears progressively over several days. Instead, we interpret this activity as the output of the SCN, which remained entrained to the LD cycle, and upon release into constant conditions, could regain control over behavioral outputs. Support for this interpretation is the fact that upon release into constant conditions from fear entrainment under DD, foraging, feeding, and, to a great extent, nest activity display no reemergence of the phase of activity before the fear presentation (Fig. 1*E* and *SI Appendix*, Fig. S2*D*). This result suggests that in the absence of an LD cycle, cyclic fear does not compete with the entrainment of the SCN by light.

Regardless of the cause for the reemergence of previous nocturnal activity, there is no doubt that the dawn activity peak that is present during the presentation of nocturnal fear represents the output of a circadian oscillator for several reasons. First and most important, the phase of the dawn peak of activity persists upon removal of the zeitgebers for all three behaviors, an outcome that defines entrainment of a circadian pacemaker (20). Second, the appearance of the dawn peak of activity when the nocturnal fear is presented displays transients; i.e., it does not appear on the first day of the presentation of shocks but it takes several days and is the result of the progressive shift in the phase of activity. This behavior is typically interpreted as the output of a circadian clock that cannot instantaneously phase-shift by several hours. Third, the dawn peak of activity in DF mice precedes the onset of the light phase and the end of the shock time window. This anticipation to a cyclic event is typically interpreted as the output of a biological clock.

Despite the discovery of the FEO over half a century ago, the basic molecular mechanisms behind this clock and its precise location in the brain or body have remained remarkably elusive (10, 21). Animals devoid of a canonical circadian molecular clock, as well as those with complete lesions of the SCN, can still entrain to restricted food access. In contrast, rats with lesions of the SCN are unable to entrain to nocturnal fear (7). In this study, we further demonstrate that a functional molecular clock within the SCN is necessary for fear entrainment. This finding potentially suggests that the SCN can be entrained by cyclic fear in a similar manner to how it is entrained by the LD cycle. However, this is likely not the case for two reasons. First, we show that when mice entrain to nocturnal fear, clock gene expression in the SCN remains synchronized to the LD cycle and not to the timing of fear. Second, animals with a functional SCN, but nonfunctional clocks in the rest of the forebrain fail to entrain to cyclic fear. This latter result suggests that other brain centers that rely on a canonical molecular circadian clock can entrain to cyclic fear. However, neither the amygdala nor the dentate gyrus exhibits synchronized clock gene expression with cyclic fear. Importantly, the rescue approach we use in the present work, based on the reconstitution of the molecular clockwork in the SCN through the constitutive expression of *Bmal1*, could never restore the function to that of an intact wild-type SCN, leaving the possibility that in intact mice the SCN central clock could be sufficient for fear entrainment. This possibility, however, would be hard to reconcile with two results. First, the pattern of clock gene expression in intact mice does not change under nocturnal fear entrainment. Second, although mice with SCN-specific *Bmal1* rescue could not entrain to cyclic fear they did entrain to an LD cycle.

The necessity, but not sufficiency, of the SCN for animals to entrain to cyclic fear suggests that its role is to convey phase information about the LD cycle. However, we also show that, remarkably, animals cannot entrain to fear without a functional SCN, even under DD. Thus, the SCN may provide an internal circadian phase reference, enabling the scheduling of foraging, feeding, and nest activity to avoid a circadian time in which a threat is present.

The discovery of circadian oscillators outside the SCN about two decades ago challenged the classic layout of a central circadian clock governing overt circadian rhythms. It soon became clear that clocks downstream of the SCN played an important role as subordinate clocks, timing local rhythmic outputs such as enzymatic

pathways in the liver or glucocorticoid production in the adrenal gland. This layout was further complicated by examples where these subordinate clocks could independently synchronize to external cycles and override central control by the SCN. For instance, restricted food access during the light phase in mice entrains the liver clock and extra-SCN oscillators in the brain but does not entrain the SCN (22–24). This change in the configuration of the ensemble of circadian oscillators is associated with daytime activity anticipating food arrival, indicating that the typical hierarchy in which the SCN is the leading oscillator timing daily activity can be altered, allowing other oscillators to take control. Similarly, our results show that cyclic aversive stimuli can entrain overt patterns of behavior, clearly indicating that fear-coding centers are an integral component of the circadian system, alongside the liver, the retina, and the central SCN pacemaker.

This notion may have significant implications for understanding symptoms of fear and anxiety disorders, which are often associated with sleep and circadian disruptions, particularly in patients suffering from posttraumatic stress disorder (PTSD). Our results show that cyclic aversive stimuli lead to changes in the circadian timing of behavior that persist even after the aversive stimulus is removed. This supports the interpretation that sleep and circadian disorders associated with PTSD could represent the output of a circadian oscillator that was previously entrained to time-specific fear.

Materials and Methods

Animals. C57BL/6 J male and female mice purchased from The Jackson Laboratory were used for all experiments carried out with wild-type mice. The light-fear (LF), dark-fear (DF), cued and noncued fear in constant darkness experiments with wild-type mice were done with male mice only. These experiments were replicated with both females and males, and all remaining experiments had approximately 50% females. For none of the reported behavioral or histological assays did sex have an effect on the outcome variables, and results represent the aggregated data of males and females. *Cami-Bmal1* mice were generated as previously described (12). Briefly, *Camk2a::iCre*BAC mice (*CamiCre*$^{+/-}$) (MGI:2181426), were crossed to *Bmal1*$^{fx/fx}$ mice (The Jackson Laboratory Stock number 007668) to produce *CamiCre*$^{+/-}$;*Bmal1*$^{fx/+}$. These animals were backcrossed to *Bmal1*$^{fx/fx}$ to produce *CamiCre*$^{+/-}$;*Bmal1*$^{fx/fx}$ (*Cami-Bmal1*$^{-/-}$), *CamiCre*$^{+/-}$;*Bmal1*$^{fx/+}$ (*Cami-Bmal1*$^{+/-}$) and *CamiCre*$^{-/-}$;*Bmal1*$^{fx/fx}$ (*Cami-Bmal1*$^{+/+}$). The *CamiCre* driver transgenic line leads to high levels of Cre expression in the hippocampus, cortex, and amygdala, lower levels in the striatum, thalamus, hypothalamus, and medulla, and no expression in the cerebellum and outside of the brain (25). Despite the overall low levels of expression in the hypothalamus, this *Camk2a::iCre* transgenic line leads to high levels of expression within SCN (unlike other *Camk2a::iCre* transgenic lines). For this reason, it is a highly convenient line to induce behavioral arrhythmia when crossed to *Bmal1*$^{fx/fx}$ transgenic mice (12). Importantly, unlike the global knock-out of the *Bmal1* gene, this approach leads to behaviorally arrhythmic mice that are healthy, have normal lifespan and no reproductive deficits (12). Because of the broad pattern of Cre expression in the Cre transgenic line, and following the same nomenclature as Izumo et al. (12), we refer to the *Cami-Bmal1*$^{-/-}$ mice as forebrain-specific *Bmal1* knock-outs.

To induce the deletion of the *Bmal1* gene specifically in the adult SCN, *Bmal1*$^{fx/fx}$ adult mice were injected bilaterally at the SCN with a Cre and GFP-expressing AAV (AAV2/1-Ef1a-Gfp-Cre).

To rescue the expression of *Bmal1* in the SCN of mice lacking its expression in the forebrain, *Cami-Bmal1*$^{-/-}$ mice were injected with a Cre-dependent *Bmal1*-expressing AAV (AAV2/1-Ef1a-DIO-Bmal1).

The viruses were produced in the Vision Core Lab at the University of Washington. The *Bmal1*-expressing plasmid was custom made by VectorBuilder (Chicago, IL). Targeted viral injections to the SCN were performed aseptically while mice were head-fixed on a stereotaxic device and anesthetized with isoflurane. The injection coordinates were: anteroposterior −0.5 mm, mediolateral ± 0.25 mm, and dorsoventral −5.65 mm. Viruses were loaded into pulled glass capillary needles that were backfilled with biologically inert Perfluro-compound (FC-770) and administered using a Nanoject II (Drummond Scientific). 500 nL of virus was injected at a working concentration of 10^{12} particles/ml to each hemisphere of the SCN.

Mice injected with viral vectors to either delete or rescue the expression of *Bmal1* from the SCN were singly housed in regular housing cages equipped with infrared detectors to record home-cage activity and screened for locomotor activity rhythms 2 wk after recovery from surgery. Then, they were subjected to the fear protocol, and after their behavior was evaluated, they were dissected, and brains stained to check for the places of injection within the hypothalamus.

For the *Bmal1* SCN-knock out (SCN-KO) experiment, only mice that displayed both an arrhythmic pattern of behavior during the screening and showed bilateral hits into SCN during the histological assessment were considered for the SCN-KO group. Mice that displayed rhythmic patterns of locomotor activity during the screening and presented no trace of the virus in the hypothalamus were considered for the analysis within the control group. Mice with unilateral or partial hits to the SCN were discarded from the analysis regardless of their pattern of behavior during the behavioral screening. Among 12 mice injected for the SCN-targeted deletion of *Bmal1*, 10 were used for the final analysis, 6 of them were arrhythmic during postsurgical behavioral screening and presented bilateral hit to the SCN, 4 of them remained rhythmic and the histology showed that the SCN was not hit by the injection and there were no trace of the virus in the hypothalamus, and 2 of them were removed from the analysis because they presented partial hits into the SCN, both of them remained rhythmic during the behavioral screening.

For the *Bmal1* rescue experiment, only mice that displayed a circadian rhythm in locomotor activity during the behavioral screening phase and showed a unilateral or bilateral hit to SCN during the histological assessment, consistent with the recovery of the locomotor activity rhythm, were considered for the SCN-*Bmal1* rescued group. Mice that displayed arrhythmic patterns of locomotor activity during the screening and presented no trace of the virus in the hypothalamus were taken into account for the analysis within the control group. Among 15 mice injected for the SCN-targeted rescue of *Bmal1*, 7 presented a rhythmic pattern of locomotor activity with a period within the circadian range and bilateral hits to the SCN, 4 a rhythmic pattern of locomotor activity with a period within the circadian range and partial or unilateral hits to the SCN, and 4 of them displayed arrhythmic locomotor activity patterns with no significant period detected in the circadian range and no trace of the injection in the hypothalamus or SCN-surrounding tissue.

Cyclic Fear Paradigm. Animals were housed in regular (19 × 40 × 18 cm W × L × D) mouse cages under a 12:12 LD cycle unless otherwise indicated. For fear-entrainment experiments, each mouse was singly housed in a fear conditioning chamber. The chamber is composed of a nesting area (11 × 21 × 20 cm W × L × H) containing corncob bedding connected to a "foraging area" (10 × 21 × 20 cm) that provided ad libitum access to food and water (*SI Appendix*, Fig. S1*A*). The floor of the foraging area consisted of a foot-shock grid that was connected to an Arduino-controlled (Arduino Uno; New York, NY) shocker that could be programmed to deliver shocks with any temporal structure. Two independent IR detectors recorded the activity within the nesting and foraging areas, respectively, and a laser bin detected nose-pokes into the food container. Thus, we continuously recorded nest activity, foraging (activity within the foraging area), and feeding for each individual animal.

The basic fear-entrainment protocol consisted of three different phases. First, a baseline phase (~14 d) in which the mice were allowed to familiarize themselves with the new environment without receiving any aversive stimulus. Second, the shocks phase (10 to 15 d), in which the aversive stimulus, three 0.2-mAmp foot shocks per hour randomly distributed, was incorporated in a daily 12-h window in a phase-specific manner (see below). During the final postshock phase (7 to 10 d), mice were released into constant darkness conditions, and the aversive stimulus was removed. This free-running phase was necessary to evaluate whether rhythmic activity as the result of the time-specific shocks was the result of circadian entrainment.

Light and Dark Fear Entrainment Protocol. In mice subjected to footshocks during the light phase (light fear = LF) protocol, the 12-h window of shock presentation was paired to the 12-h light phase of the LD cycle. For mice subjected to footshocks during the dark phase (dark fear = DF), the stimulus was presented in the opposite phase, paired with the 12-h dark phase.

Cued and Noncued Constant Darkness Fear Entrainment Protocol. Mice were first placed in the fear chamber under an LD cycle for a minimum of 7 d and were subsequently transferred into DD (dim red light of <2-lux intensity). After

a 14-d-long baseline phase, one group of animals received a 12-h window of shocks with the same temporal structure as above (noncued fear group) whereas the second group received the same temporal pattern of shocks but each shock was preceded by a 20-s 4 kHz 75 dB tone that served as the conditioned stimulus (cued fear group).

In Situ Hybridization. Mice were subjected to a baseline phase (10 d) followed by either LF or DF phases (15 d) (as described in the LD protocol above). During the last day of shock exposures, mice were killed and their brains collected and frozen every 4 h for 24 h (ZT 2, 6, 10, 14, 18, 22). Frozen brains were sliced in 16-μm-thick coronal slices by using a cryostat and mounted on Vectabond-treated slides. In situ hybridization for *Per1* and *Bmal1* genes was conducted as previously described (26, 27). Autoradiographic images were generated by exposing slides to Ultramax film (Kodak, Rochester, NY). Images were scanned at high resolution, and hybridization intensities were determined with ImageJ software (NIH, Bethesda, MD).

Immunohistochemistry. Brain tissue for immunohistochemistry (IHC) was harvested at ZT 9–11 under LD 12:12 conditions. Briefly, mice were anesthetized with Isoflurane and perfused transcardially using 0.01 M phosphate-buffered saline followed by 4% paraformaldehyde in 0.1 M phosphate buffer. Brains were removed and postfixed overnight at 4 °C in 4% paraformaldehyde in 0.1 M phosphate buffer and then incubated at 4 °C in 30% sucrose/phosphate buffer overnight.

Cryostat 30-μm coronal sections were collected into three alternate sets representing the whole rostro-caudal extent of the SCN and used for free-floating IHC. Briefly, the slices were incubated in 0.4% tween 20 in 0.01 M phosphate-buffered saline (PBST) for 15 min to permeabilize tissue and then blocked in 5% donkey serum in PBST for an hour. After a quick rinse in 0.04% PBST, the slices were incubated in BMAL1 (1:1,000, Novus Biological cat# NB100-2288) primary antibody solution at 4 °C overnight. Then, the slices were washed four times, 10 min each in 0.04% PBST and incubated in Alexa 594 Donkey anti-Rabbit secondary antibody diluted in 0.04% PBST (1:300, Invitrogen cat# A21207) for 2 h at room temperature. After the secondary antibody incubation, the slices were washed four times, 5 min each with 0.04% PBST, and mounted into glass slides and coverslipped with DAPI Fluoromount-G (Southern Biotech, Birmingham, AL).

Images were taken using a Leica TCS SP5 II laser scanning confocal microscope (20X objective) in 1-μm Z-stacks using identical capture settings for every slice.

Statistical Analysis of Behavioral Outputs

Average daily activity patterns (or "waveforms") of the different outputs measured were generated using 7 d of recording for each stage in the fear entrainment protocol (the last 7 d for baseline and shocks phases, and the first 7 d of postshocks phase). The percentage of activity performed during the light phase for experiments carried under LD conditions, and the percentage of activity displayed during the safe phase (no-shocks) in DD conditions were calculated using El Temps software (University of Barcelona, Spain). The onset of activity was calculated using El Temps software and those phases were evaluated using the Rayleigh test.

To evaluate the robustness of the rhythms in the behavioral outputs measured, the relative power from the FFT for the peak within the circadian range (20 to 28 hs) was measured for each mouse (Clocklab Analysis, Actimetrics) and used for statistical analysis.

Linear mixed-effects models (LMM) were used to analyze differences in the percent of locomotor and feeding activity at specific phases, and in FFT power across the protocol stages using the lme4 package for R (28). Statistical significance for LMM factors was calculated through a Type III analysis using Satterthwaite's method using the lmerTest package (29). Post hoc Tukey comparisons within groups were performed using the emmeans package (30).

Expression of genes measured by in situ hybridization were fit to a cosinor model, and differences in fit parameters were analyzed through Wald tests using the cosinor package for R (31).

Group-wise average activity patterns were calculated and plotted using a locally estimated scatterplot smoothing (LOESS) using tools from the tidyverse-package for R (32).

Data, Materials, and Software Availability. Data used to generate figures data have been deposited in GitHub (https://github.com/delaiglesialab/Bussi-et-al.-PNAS-2024/) (33).

ACKNOWLEDGMENTS. NIH grant R01NS110012 and R01NS108934 (H.O.d.l.I.). NIH grant EY07031 and EY001730.

Author affiliations: [a]Department of Biology, University of Washington, Seattle, WA 98195-1800; [b]Molecular & Cellular Biology Graduate Program, University of Washington, Seattle, WA 98195-7275; [c]Department of Neuroscience, University of Texas Southwestern Medical Center, Dallas, TX 75390-9111; [d]HHMI, Chevy Chase, MD 20815; and [e]Department of Psychology, University of Washington, Seattle, WA 98195-1525

1. J. Ross, A. J. Hearn, P. J. Johnson, D. W. Macdonald, Activity patterns and temporal avoidance by prey in response to Sunda clouded leopard predation risk. *J. Zool.* **290**, 96–106 (2013).
2. V. van der Vinne *et al.*, Maximising survival by shifting the daily timing of activity. *Ecol. Lett.* **22**, 2097–2102 (2019).
3. M. G. P. Fenn, D. W. Macdonald, Use of middens by red foxes: Risk revereses rhythms of rats. *J. Mamm.* **76**, 130–136 (1995).
4. H. M. Swarts, K. R. Crooks, N. Willits, R. Woodroffe, Possible contemporary evolution in an endangered species, the Santa Cruz Island fox. *Anim. Conserv.* **12**, 120–127 (2009).
5. N. Kronfeld-Schor, M. E. Visser, L. Salis, J. A. van Gils, Chronobiology of interspecific interactions in a changing world. *Philos. Trans. R. Soc. Lond. B Biol. Sci.* **372**, 20160248 (2017).
6. M. C. Hernández *et al.*, Behavioral responses of wild rodents to owl calls in an austral temperate forest. *Animals (Basel)* **11**, 428 (2021).
7. B. A. Pellman *et al.*, Time-specific fear acts as a non-photic entraining stimulus of circadian rhythms in rats. *Sci. Rep.* **5**, 14916 (2015).
8. D. K. Welsh, J. S. Takahashi, S. A. Kay, Suprachiasmatic nucleus: Cell autonomy and network properties. *Annu. Rev. Physiol.* **72**, 551–577 (2010).
9. C. L. Partch, C. B. Green, J. S. Takahashi, Molecular architecture of the mammalian circadian clock. *Trends Cell Biol.* **24**, 90–99 (2014).
10. R. E. Mistlberger, Neurobiology of food anticipatory circadian rhythms. *Physiol. Behav.* **104**, 535–545 (2011).
11. K. F. Storch, C. J. Weitz, Daily rhythms of food-anticipatory behavioral activity do not require the known circadian clock. *Proc. Natl. Acad. Sci. U. S. A.* **106**, 6808–6813 (2009).
12. M. Izumo *et al.*, Differential effects of light and feeding on circadian organization of peripheral clocks in a forebrain Bmal1 mutant. *eLife* **3**, e04617 (2014).
13. A. Padlom *et al.*, Level of constitutively expressed BMAL1 affects the robustness of circadian oscillations. *Sci. Rep.* **12**, 19519 (2022).
14. A. C. Liu *et al.*, Redundant function of REV-ERBalpha and beta and non-essential role for Bmal1 cycling in transcriptional regulation of intracellular circadian rhythms. *PLoS Genet.* **4**, e1000023 (2008).
15. E. L. McDearmon *et al.*, Dissecting the functions of the mammalian clock protein BMAL1 by tissue-specific rescue in mice. *Science* **314**, 1304–1308 (2006).
16. R. A. Hut, N. Kronfeld-Schor, V. van der Vinne, H. O. de la Iglesia, In search of a temporal niche: Environmental factors. *Prog. Brain Res.* **199**, 281–304 (2012).
17. A. Castillo-Ruiz, M. J. Paul, W. J. Schwartz, In search of a temporal niche: Social interactions. *Prog. Brain Res.* **199**, 267–280 (2012).
18. F. K. Stephan, J. M. Swann, C. L. Sisk, Anticipation of 24-hr feeding schedules in rats with lesions of the suprachiasmatic nucleus. *Behav. Neural Biol.* **25**, 346–363 (1979).
19. J. R. Trzeciak, A. D. Steele, Studying food entrainment: Models, methods, and musings. *Front. Nutr.* **9**, 998331 (2022).
20. C. H. Johnson, J. A. Elliott, R. Foster, Entrainment of circadian programs. *Chronobiol. Int.* **20**, 741–774 (2003).
21. R. E. Mistlberger, Food as circadian time cue for appetitive behavior. *F1000Res* **9**, F1000 Faculty Rev-61 (2020).
22. F. Damiola *et al.*, Restricted feeding uncouples circadian oscillators in peripheral tissues from the central pacemaker in the suprachiasmatic nucleus. *Genes Dev.* **14**, 2950–2961 (2000).
23. J. Mendoza, Circadian clocks: Setting time by food. *J. Neuroendocrinol.* **19**, 127–137 (2007).
24. A. Mukherji *et al.*, Shifting eating to the circadian rest phase misaligns the peripheral clocks with the master SCN clock and leads to a metabolic syndrome. *Proc. Natl. Acad. Sci. U.S.A.* **112**, E6691–E6698 (2015).
25. E. Casanova *et al.*, A CamKIIα iCre BAC allows brain-specific gene inactivation. *Genesis* **31**, 37–42 (2001).
26. S. Han *et al.*, NaV1.1 channels are critical for intercellular communication in the suprachiasmatic nucleus and for normal circadian rhythms. *Proc. Natl. Acad. Sci. U. S. A.* **109**, E368–E377 (2012).
27. H. O. de la Iglesia, "In situ hybridization of suprachiasmatic nucleus slices" in *Methods Mol. Biol.*, E. Rosato, Ed. (Humana Press, Totowa, NJ, 2007), vol. 362, pp. 513–531.
28. D. Bates, M. Maechler, B. Bolker, S. Walker, Fitting Linear mixed-effects models using lme4. *J. Stat. Software* **67**, 1–48 (2015).
29. A. Kuznetsova, P. B. Brockhoff, R. H. B. Christensen, lmerTest package: Tests in linear mixed effects models. *J. Stat. Software* **82**, 1–26 (2017).
30. R. Lenth *et al.*, emmeans: Estimated marginal means, aka least-squares means (2020). https://cran.r-project.org/web/packages/emmeans/index.html. Accessed 20 November 2023.
31. M. Sachs, Tools for estimating and predicting the cosinor model. R package version 1.2.2 (2023). https://CRAN.R-project.org/package=cosinor. Accessed 20 November 2023.
32. H. Wickham *et al.*, Welcome to the tidyverse. *J. Open Source Software* **4**, 1686 (2019).
33. I. L. Bussi, H. O. de la Iglesia, Bussi-et-al.-2024. (Github.com) (2024). https://github.com/delaiglesialab/Bussi-et-al.-PNAS-2024/. Accessed 7 March 2024.